Diagn Interv Radiol 2025; DOI: 10.4274/dir.2025.253391

BREAST IMAGING

ORIGINAL ARTICLE

Comparison of changes in dynamic contrast-enhanced magnetic resonance imaging and flourine-18 fluorodeoxyglucose positron emission tomography/computed tomography parameters from baseline to post-neoadjuvant therapy in predicting pathological response in breast cancer

Hüseyin Akkaya[1]
Aygül Polat Kelle[2]
Tuba Dalgalar Akkaya[3]
Selim Özdemir[4]
Kübra Karaaslan Erişen[5]
Bozkurt Gülek[5]

[1]Ondokuz Mayıs University Faculty of Medicine, Department of Radiology, Samsun, Türkiye

[2]University of Health Sciences Türkiye, Adana City Training and Research Hospital, Clinic of Nuclear Medicine, Adana, Türkiye

[3]Samsun University Faculty of Medicine, Department of Radiology, Samsun, Türkiye

[4]Düziçi State Hospital, Clinic of Radiology, Osmaniye, Türkiye

[5]University of Health Sciences Türkiye, Adana City Training and Research Hospital, Clinic of Radiology, Adana, Türkiye

Corresponding author: Hüseyin Akkaya

E-mail: dr.hsynakkaya@gmail.com

Received 14 April 2025; revision requested 10 June 2025; last revision received 22 June 2025; accepted 21 July 2025.

Epub: 18.08.2025

Publication date:

DOI: 10.4274/dir.2025.253391

PURPOSE

This study aimed to compare the value of differences (Δ) in parameters obtained via both dynamic contrast-enhanced (DCE) magnetic resonance imaging (MRI) and flourine-18 fluorodeoxyglucose positron emission tomography/computed tomography (^{18}F-FDG PET/CT) between baseline and post-neoadjuvant therapy in predicting the pathological response to neoadjuvant therapy in breast cancer.

METHODS

A total of 109 patients who underwent both baseline and post-neoadjuvant therapy DCE-MRI and ^{18}F-FDG PET/CT examinations were retrospectively analyzed. The DCE-MRI parameters and ^{18}F-FDG PET/CT parameters [metabolic tumor volume (MTV), standardized uptake value $(SUV)_{max}$, SUV_{mean}, and total lesion glycolysis] were recorded at both time points. Additionally, the Δs between these parameters were calculated. Postsurgical pathology reports were documented, and the patients were subsequently categorized into two groups: those exhibiting pathologic complete response (pCR) and those exhibiting partial response. Parameters from DCE-MRI and ^{18}F-FDG PET/CT were compared to determine which predicted pathological response to neoadjuvant therapy more effectively.

RESULTS

Patients with partial response demonstrated a higher rate of histologic grade 3 than those with pCR ($P = 0.030$). The only DCE-MRI parameter to indicate a significant difference between the two groups ($P = 0.024$) was the Δ(%)wash-out rate. Among the baseline parameters, only MTV successfully predicted pathological response ($P = 0.033$). The only post-neoadjuvant therapy parameter to be predictive of pathological response ($P = 0.003$) was SUV_{mean}. In receiver operating characteristic analysis, ΔSUV_{mean} emerged as the most significant parameter for predicting pathological response, followed by post-neoadjuvant SUV_{mean} [area under the curve: 0.724 (95% confidence interval: 0.630–0.805) and 0.673 (0.577–0.760), respectively].

CONCLUSION

The Δ^{18}F-FDG PET/CT parameters are better than ΔDCE-MRI in predicting pathologic response to neoadjuvant therapy. Among these parameters, ΔSUV_{mean} is the most successful.

CLINICAL SIGNIFICANCE

Neoadjuvant chemotherapy (NAC) response is one of the most important criteria in breast cancer prognosis. The two most important imaging modalities in breast cancer diagnosis and follow-up protocols are MRI and ^{18}F-FDG PET/CT. However, it is not clear which of these two modalities is more successful in predicting the difference in treatment response between baseline and post-NAC.

KEYWORDS

Breast cancer, metabolic tumor volume, total lesion glycolysis, dynamic magnetic resonance imaging, positron emission tomography

You may cite this article as: Akkaya H, Polat Kelle A, Dalgalar Akkaya T, Özdemir S, Karaaslan Erişen K, Gülek B. Comparison of changes in dynamic contrast-enhanced magnetic resonance imaging and flourine-18 fluorodeoxyglucose positron emission tomography/computed tomography parameters from baseline to post-neoadjuvant therapy in predicting pathological response in breast cancer. *Diagn Interv Radiol*. 18 August 2025 DOI: 10.4274/dir.2025.253391 [Epub Ahead of Print].

Breast cancer is a significant public health concern, and women in particular face high breast cancer incidence and mortality rates.[1] Prognostic factors are critical for estimating recurrence risk and providing increasingly personalized treatment for patients.[2] Current therapeutic approaches in breast cancer focus on neoadjuvant chemotherapy (NAC)–also referred to as primary or induction chemotherapy–which is administered prior to surgical intervention.[3] Histological response following NAC remains the most important factor associated with recurrence risk.[2-4] In addition, early prediction of NAC response can reduce patient costs and protect patients from unnecessary side effects and time loss, leading to the use of alternative methods. Therefore, additional and more precise methods of predicting NAC response and estimating prognosis are necessary.

Although novel imaging parameters have been developed to characterize the biological features of breast tumors, factors affecting the quality of the therapeutic response remain uncertain.[5,6] Dynamic contrast-enhanced (DCE) magnetic resonance imaging (MRI) shows tissue vascularity and perfusion due to blood flow by analyzing signal intensity.[7] Semi-quantitative parameters derived from DCE-MRI can be calculated based on the signal intensity curve.[8] Although studies investigating the relationship between these semi-quantitative parameters and therapeutic responses in various tumor tissues are not uncommon in the literature,[7-9] research examining the relationship of the differences (Δ) in these parameters between diagnosis and post-neoadjuvant therapy with NAC response remains limited.

Main points

- Of the dynamic contrast-enhanced magnetic resonance imaging parameters, only Δ(%) wash-out values differed between the two groups with pathologic complete response (pCR) and partial response, with higher Δ(%) wash-out in the pCR group ($P = 0.024$).
- Delta standardized uptake value (ΔSUV_{mean}) demonstrated the best diagnostic test performance at predicting treatment response among these parameters [area under the curve: 0.724 (95% confidence interval: 0.630–0.805)].
- Metabolic tumor volume (MTV), SUV_{mean}, ΔMTV, ΔSUV_{mean}, ΔSUV_{mean}, delta total lesion glycolysis (ΔTLG), and Δwash-out values after neoadjuvant treatment and the distribution between groups were similar.
- In patients with pCR, baseline MTV, Δ(%) MTV, Δ(%) SUV_{mean}, and Δ(%) TLG values were significantly higher, whereas post-neoadjuvant chemotherapy SUV_{mean} values were significantly lower than those with a partial response.

Flourine-18 fluorodeoxyglucose positron emission tomography/computed tomography (^{18}F-FDG PET/CT) is a valuable tool in the staging of breast cancer at diagnosis and in evaluating therapeutic response and suspicion of recurrence using standardized uptake value (SUV) and its associations with various predictive and prognostic factors.[10] The SUV_{max} parameter corresponds to the point with the highest SUV value measured within a region of interest (ROI); in other words, it defines the most active part of the tumor and does not provide insight into the overall tumor status. Metabolic tumor volume (MTV) and total lesion glycolysis (TLG) have been introduced as semi-quantitative measures of ^{18}F-FDG uptake within a heterogeneous tumor mass. The MTV represents the volume of tumoral tissue demonstrating a specific ^{18}F-FDG uptake activity beyond the intensity of FDG uptake by tumor tissues.[11] Several studies have also compared the efficacy of TLG with that of MTV in predicting therapeutic responses.[2,10,11]

This study aims to evaluate whether semi-quantitative ΔDCE-MRI parameters and Δ^{18}F-FDG PET/CT indices (ΔMTV, ΔSUV_{max}, ΔSUV_{mean}, and ΔTLG) could predict pathological responses to NAC in patients with breast cancer during initial staging. These parameters are also compared with other predictive and prognostic factors [age, cellular proliferation index, histologic grade, hormone receptor expression, and human epidermal growth factor receptor 2 (HER2) status] in terms of the pathological response after NAC.

Methods

Patient selection and study design

The present study was conducted in full accordance with the guidelines of the Declaration of Helsinki, revised in 2000 in Edinburgh. Approvals for the study were obtained from the Ethics Committee of University of Health Sciences Turkey, Adana City Training and Research Hospital and the Turkish Ministry of Health (28.03.2024/3232). The requirement for informed consent from the patients was waived due to the retrospective nature of the study. Of the 262 cases diagnosed during this period, 109 female patients who underwent both preoperative DCE breast MRI and ^{18}F-FDG PET/CT at both diagnosis and after the completion of NAC were included in the study, following the application of the exclusion criteria (Figure 1). All patients underwent clinical tumor staging via baseline clinical examination, mammography, and ultrasonography along with a tru-cut biopsy. Both ^{18}F-FDG PET/CT and cranial MRI examinations were performed for tumor–node–metastasis staging. To avoid the partial volume effect during measurement of ^{18}F-FDG PET/CT uptake, all lesions in the study had a long axis >15 mm.

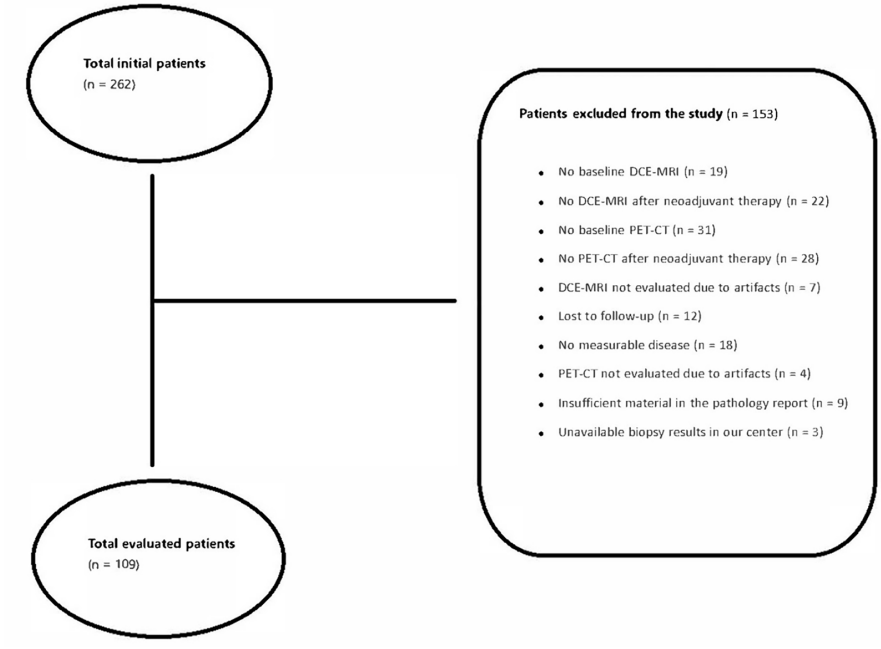

Figure 1. Flowchart of the study. DCE, dynamic contrast-enhanced; MRI, magnetic resonance imaging; PET-CT, positron emission tomography-computed tomography.

Semi-quantitative parameters from DCE-MRI at the time of diagnosis were recorded. Subsequently, semi-quantitative DCE-MRI parameters obtained after NAC were documented, including (1) maximum enhancement, (2) maximum relative enhancement, (3) T0 (s), (4) time to peak (s), (5) wash-in rate (s^{-1}), and (6) wash-out rate (s^{-1}). Differences between the measurements obtained at diagnosis and those recorded after NAC were calculated. Additionally, the SUV_{max}, SUV_{mean}, TLG, and MTV values obtained from ^{18}F-FDG PET/CT at diagnosis and after NAC were recorded, and the Δs between these parameters were calculated. The percentage changes (Δ%) for all ^{18}F-FDG PET/CT and MRI parameters were calculated using the following formula:

Percentage change (Δ%) = (delayed parameter − baseline parameter) / baseline parameter × 100.

Magnetic resonance imaging acquisition

The MRI protocols for this study adhered to the standards established by the breast MRI accreditation program of the American College of Radiology.[12] A three-dimensional T1-weighted fast gradient echo-based DCE series with one pre-contrast and three sequential post-gadolinium contrast-enhanced sequences, each with a scan duration of approximately 3 minutes, was imaged. The examinations were conducted using a 3-Tesla scanner (Ingenuity; Philips Healthcare, the Netherlands) with a 16-channel breast coil. The DCE-MRI was performed using a fat-saturated three-dimensional fast gradient echo sequence with the following parameters: repetition time/echo time, 5.8/3 ms; flip angle, 15°; spatial resolution, 0.5 × 0.6 × 1.4 mm; voxel size, 0.8 × 0.8 × 2; temporal resolution, 60 s; number of sections, 200; and field of view, 360 × 360 mm. Fat suppression was achieved via the short-scar periareolar inferior pedicle reduction technique. All images were acquired in axial orientation. The contrast agent used was gadobutrol (Gadovist, Bayer Schering Pharmaceuticals, Mississauga, Canada) administered at a dose of 0.1 mmol/kg body weight and a rate of 2 cc/s, followed by a 15 cc saline flush.

Magnetic resonance imaging evaluation

All obtained DCE-MRI were retrospectively reviewed based on consensus by two experienced radiologists with 9 and 7 years of experience in breast MRI. The radiologists were blinded to clinicopathological findings and clinical follow-up data except for data on the presence of breast cancer. All images obtained using the software were analyzed. Regions of interest were defined as areas demonstrating abnormal signals on the MRI and were manually delineated using the oval-shaped function (Figure 2). Time–intensity curves and time-to-peak values were automatically generated based on these ROIs.

In accordance with previously published methodologies, multiple circular ROIs measuring 25 mm^2 (approximately 5.6 mm in diameter) were carefully placed within the solid portion of the tumor, as indicated by DCE-MRI and T2-weighted imaging.[2,7,9] The ROIs were meticulously positioned within the tumor to avoid cystic regions or visual artifacts, and average values within each ROI were recorded. These analyses were performed using a dedicated workstation (IntelliSpace, Philips, Netherlands).

Acquisition of flourine-18 fluorodeoxyglucose positron emission tomography/computed tomography

Patients were placed in the supine position during imaging, and CT transmission scanning was performed without intravenous contrast enhancement. The scan utilized a low tube current (135 kVp, 46–79 mAs), a slice thickness of 4.0 mm, a gantry rotation of 0.53 s, and a collimator width of 5 × 3 mm. Following a minimum fasting period of 6 hours, an intravenous injection of 370–555 MBq ^{18}F-FDG was administered. Whole-body images were acquired using a PET/CT scanner (Ingenuity; Philips Healthcare, the Netherlands) 40–60 minutes after injection. Visual analysis employed a four-point certainty scoring system (definitely negative, equivocal: probably negative, equivocal: probably positive, and definitely positive) and included assessments of anatomical site and lesion size. The emission data were acquired for 2.5 min per bed (six to seven beds), which were later attenuation-corrected with the digital CT data. Image reconstruction used the ordered subsets expectation maximization algorithm of two iterations and eight subsets.

Flourine-18 fluorodeoxyglucose positron emission tomography/computed tomography evaluation

All ^{18}F-FDG PET/CT images were retrospectively evaluated by a nuclear medicine specialist with 17 years of experience in PET-CT. This specialist was blinded to clinicopathological and clinical follow-up data that did not cover the presence of breast cancer. The foci of FDG uptake were identified if FDG accumulation exceeded that of comparable normal contralateral or surrounding tissues. The workstation automatically generated SUV_{max}, SUV_{mean}, and MTV (cm^3) from the volume of interest (VOI) (Figure 3). The target lesion margins inside the VOI were also automatically defined, and voxels exceeding 41% of the SUV_{max} within the VOI were included in the MTV and SUV_{mean} calculations. Among the relative thresholds of 40% SUV_{max} for tumor delineation and contouring on PET/CT in patients with breast cancer, it is the most appropriate and popular cut-off value and prognostic marker.[1-4] The TLG was calculated

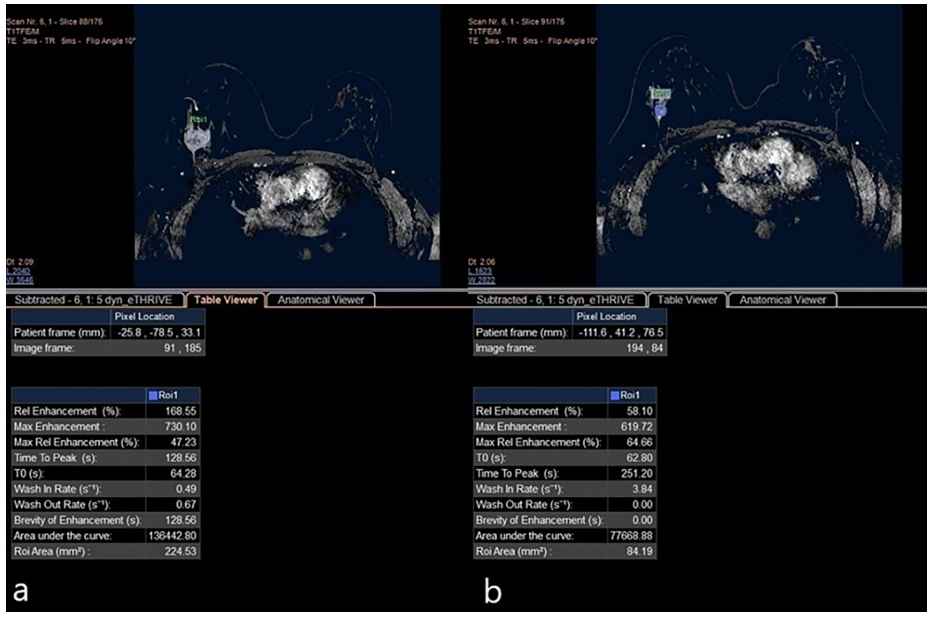

Figure 2. Changes in dynamic contrast-enhanced magnetic resonance imaging baseline **(a)** and post-neoadjuvant therapy **(b)** parameters of the same patient. Although there was a significant change in all dynamic parameters in this patient, the pathology result was a partial response.

by multiplying MTV by SUV_{mean}. Due to the study's retrospective nature, semi-quantitative measurements were retrospectively reproduced by the nuclear medicine specialist taking part in the study, who was blinded to all other data.

Chemotherapy regimen and histological evaluation

The NAC regimens included combinations such as doxorubicin and cyclophosphamide, doxorubicin and cyclophosphamide followed by taxane, doxorubicin and docetaxel, and taxane combined with anti-HER2 agents.

The pathological characteristics of the tumors examined in this work, including their histological type, histological grade, Ki67 proliferation index, hormone receptor expression, and HER2 status, were analyzed based on biopsies obtained at diagnosis prior to NAC. Immunohistochemical (IHC) analysis was used to determine whether the tumor tissue was positive or negative for HER2 and hormone receptors [estrogen receptor (ER) and progesterone receptor (PR)]. For hormone receptor expression positivity, ≥10% was accepted. The HER2 expression results were grouped as negative, 1+, 2+, or 3+. Then, the fluorescence *in situ* hybridization (FISH) method was used for gene amplification in cases with HER2 IHC staining score 2+. Cases with an IHC staining score of 3+ were defined as HER2 positive, or in the case of an IHC staging score of 2+, FISH positive.The Elston and Ellis[13] criteria (grades 1, 2, and 3) were used to determine histological grades. The IHC study of the tumor tissue obtained positive or negative results for ER and PR and stratified these results according to the modified Allred scale.[14] Histological responses to antibodies in the breast were assessed using Miller–Payne grading.[15] Pathologic complete response (pCR) is defined as the complete disappearance of cancer cells on histopathologic examination of mastectomy material after neoadjuvant treatment. Since the presence of residual ductal carcinoma *in situ* (DCIS) has prognostic significance and affects the comparability of the results with other studies, in this study, the pCR group was considered to be the absence of any tumor cells, including DCIS. The patients were categorized into five subgroups based on the recommendations of the 12th International Breast Conference: (1) luminal A; (2) luminal B-HER2(–); (3) luminal B-HER2(+); (4) HER2(+); (5) triple-negative.[16] The threshold for Ki67 positivity was 14%.

Statistical analysis

Statistical analysis was conducted using SPSS version 23.0 statistical software (SPSS, Chicago, IL, USA). Categorical variables were summarized as counts and percentages, and continuous variables were presented as means and standard deviations or medians (Q1–Q3) where applicable. Comparisons of categorical variables were conducted using the chi-squared test. The Kolmogorov–Smirnov test was applied to assess the normality of parameter distributions. For non-normally distributed parameters, the Mann–Whitney U test was employed. The sensitivity and specificity of the relevant parameters in predicting patient response to treatment were calculated. Moreover, the area under the receiver operating characteristic curve (AUC) was analyzed to determine the cut-off values. A P value of <0.05 was considered statistically significant in all tests.

Results

The rate of patients with histological grade 3 was found to be higher in those exhibiting a partial response than those achieving pCR ($P = 0.030$). No significant differences were observed between the treatment groups in relation to the remaining parameters ($P > 0.05$) (Table 1).

In patients with pCR, baseline MTV, Δ(%)MTV, Δ(%)SUV_{mean}, and Δ(%)TLG values were significantly higher ($P = 0.033$; $P = 0.014$; $P < 0.001$; and $P = 0.014$, respectively), whereas post-NAC SUV_{mean} values were significantly lower than those with a partial response ($P = 0.003$) (Table 2).

Tumor size and/or changes in tumor size were not associated with response to NAC. However, patients who achieved pCR exhibited significantly higher Δ(%)wash-out values ($P = 0.024$). No significant differences were observed between the two groups in terms of the remaining DCE-MRI parameters (Table 3).

Baseline MTV (AUC: 62.5%), post-NAC SUV_{mean} (AUC: 67.3%), ΔMTV (AUC: 64.5%), ΔSUV_{mean} (AUC: 72.4%), ΔTLG (AUC: 64.4%), and the DCE-MRI parameter Δwash-out (AUC: 63.5%) were found to be statistically significant predictors of treatment response ($P < 0.05$). The ΔSUV_{mean} parameter demonstrat-

Table 1. Comparison of demographic and pathological findings between the two groups

	Partial response (n = 72) n (%)	pCR (n = 37) n (%)	*P* value
Age (years), median (range)	47 (25–70)	53 (34–72)	0.345
Lymphovascular invasion	28 (38.9)	11 (29.7)	0.345
Histological grade			
1	34 (47.2)	12 (32.4)	**0.030***
2	22 (30.6)	22 (62.2)	
3	16 (22.2)	3 (5.4)	
CERB2			
0	12 (16.7)	9 (24.3)	0.355
1	12 (16.7)	6 (16.2)	
2	37 (51.4)	13 (35.1)	
3	11 (15.3)	9 (24.3)	
High Ki67 expression	45 (62.5)	20 (54.1)	0.395
ER	54 (75)	30 (81.1)	0.475
PR	44 (61.1)	23 (62.2)	0.915
HER2	25 (34.7)	13 (35.1)	0.966
Luminal A	15 (20.8)	10 (27.0)	0.801
Luminal B HER2-negative	26 (36.1)	12 (32.4)	0.677
Luminal B HER2-positive	18 (25.0)	11 (29.7)	0.597
HER2-positive	7 (9.7)	2 (5.4)	0.438
Triple-negative	6 (8.3)	2 (5.4)	0.579

*$P < 0.05$, chi-squared test. pCR, pathological complete response; ER, estrogen receptor; PR, progesterone receptor; HER2, human epidermal growth factor receptor 2.

ed the best diagnostic test performance at predicting treatment response among these parameters, with a cut-off value of >30.5 and an AUC of 72.4 (Table 4).

The MTV, SUV_{mean}, ΔMTV, ΔSUV_{mean}, ΔSUV_{mean}, ΔTLG, and Δwash-out values after neoadjuvant treatment and the distribution between biological subtypes were similar (P = 0.837; P = 0.325; P = 0.897; P = 0.664; P = 0.782; P = 0.425, respectively) (Figure 4).

Discussion

The response to NAC is the most significant parameter for predicting breast cancer prognosis.[17,18] Therefore, the ability to predict the response to NAC can be considered equivalent to anticipating the course and prognosis of the disease.[19] DCE breast MRI and ^{18}F-FDG PET/CT are the two most utilized imaging modalities for patients with breast cancer worldwide. Therefore, the current study aimed to identify the most effective parameter among these two imaging techniques for predicting the response to NAC.

Although SUV is a widely accepted parameter in clinical practice, SUV_{max} remains controversial.[20] This is because SUV_{max} reflects the single-pixel value of the maximum intensity of ^{18}F-FDG activity rather than the entire tumor mass. Furthermore, SUV_{max} is affected by body weight.[21] In the current study, no SUV_{max} value (baseline, post-NAC, or Δ) successfully predicted the response to NAC. On the other hand, SUV_{mean}, as an average measurement, avoids these limitations. Accordingly, ΔSUV_{mean} and post-NAC SUV_{mean} were determined to be the most valuable ^{18}F-FDG PET/CT parameters for predicting histopathological response in this study.

By adjusting for lean body mass, MTV reflects metabolic activity across the entire tumor mass.[22,23] In addition, MTV appears to be correlated with total tumor burden and tumor aggressiveness in various solid tumors, thus providing useful prognostic information.[24] Both TLG and MTV are volumetric parameters used to estimate total radioactivity within a tumor above a set threshold.[25] They have both proven to be useful in assessing the therapeutic effects and prognosis of chemotherapy.[26] The size of the tumor is also included in the calculation of TLG and MTV. It is not surprising that TLG and MTV increase with increasing tumor size, as found in some recent studies. In addition, some studies have shown that poorly differentiated tumors have significantly higher TLG and larger MTV than well-differentiated tumors.[27,28] In this study, both ΔMTV and baseline MTV predicted response to NAC, whereas MTV after

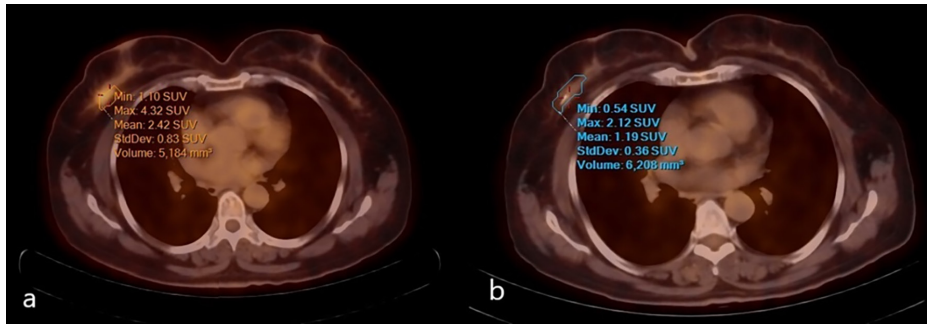

Figure 3. Changes in flourine-18 fluorodeoxyglucose positron emission tomography/computed tomography parameters at **(a)** baseline and **(b)** after neoadjuvant treatment of the same patient. This patient, whose ΔSUV_{max}, ΔSUV_{mean} changes were evident, had a pathologic complete response according to pathology. SUV, standardized uptake value.

Table 2. Comparison of flourine-18 fluorodeoxyglucose positron emission tomography/computed tomography parameters and Δ(%) values between the two groups

	Partial response (n = 72)	pCR (n = 37)	*P* value
	Median (Q1–Q3)	Median (Q1–Q3)	
Baseline MTV (cc)	155 (84–254)	19.2 (11.9–44.8)	**0.033***
Post-NAC MTV (cc)	387 (305–532)	4.25 (2.68–6.4)	0.659
ΔMTV (%)	683 (541–835)	82.3 (67–90.8)	**0.014***
Baseline SUV_{max}	742 (5.21–122)	8.19 (5.42–22.69)	0.206
Post-NAC SUV_{max}	328 (2.98–452)	3.69 (2.78–4.98)	0.554
ΔSUV_{max} (%)	517 (295–663)	59.8 (37.7–77.8)	0.192
Baseline SUV_{mean}	3.89 (3.1–7.27)	4.15 (3.1–9.19)	0.481
Post-NAC SUV_{mean}	3.05 (2.45–3.65)	2.17 (1.73–3.18)	**0.003****
ΔSUV_{mean} (%)	26.4 (19.6–43.2)	48.9 (32.6–64.9)	**<0.001****
Baseline TLG	61.8 (29.4–154.3)	117.9 (41.2–293.4)	0.051
Post-NAC TLG	11.5 (7.42–18.73)	11.9 (6.36–29.7)	0.687
ΔTLG (%)	79.1 (65.4–90.3)	88.2 (75.2–94.1)	**0.014***

*P < 0.05, **P < 0.01, Mann–Whitney U test. MTV, metabolic tumor volume; SUV, standardized uptake value; TLG, total lesion glycolysis; pCR, pathologic complete response; NAC, neoadjuvant chemotherapy.

Table 3. Comparison of dynamic contrast-enhanced magnetic resonance imaging parameters and Δ(%) values between the two groups

	Partial response (n = 72)	pCR (n = 37)	*P* value
	Median (Q1–Q3)	Med (Q1–Q3)	
Baseline tumor size on MRI (mm)	36 (29–45)	36 (22–52)	0.773
Post-NAC tumor size on MRI (mm)	19 (14–26)	20 (14–27)	0.875
ΔTumor size on MRI (mm)	45.1 (27.8–60)	47.6 (31–62.4)	0.569
Baseline maximum enhancement	963 (786–1080)	952 (711–1023)	0.113
Post-NAC maximum enhancement	442 (214–768)	475 (254–672)	0.766
ΔMaximum enhancement (%)	55.4 (18.6–77.9)	41.8 (14.6–71.4)	0.768
Baseline maximum reel enhancement	51 (44–58)	52 (41–59)	0.820
Post-NAC maximum reel enhancement	32 (12–50)	29 (12–46)	0.883
ΔMaximum reel enhancement	37.2 (2.5–74.5)	25.4 (11.5–76.9)	0.825
Baseline TTP	139 (124–163)	154 (124–188)	0.355
Post-NAC TTP	168 (140–187)	174 (144–192)	0.238
ΔTTP (%)	-13.9 (-40.3–11)	-3.03 (-46.9–13.5)	0.908
Baseline wash-in	5.86 (4.05–7.88)	5.56 (3.75–7.44)	0.957
Post-NAC wash-in	3.42 (1.69–6.2)	3.71 (2.3–4.67)	0.683
ΔWash-in (%)	23.4 (-5.6–68.3)	38.7 (17.8–60.9)	0.754
Baseline wash-out	0.55 (0.23–1.58)	0.67 (0.36–1.84)	0.129
Post-NAC wash-out	0.3 (0.18–1.1)	0.25 (0.14–0.54)	0.118
ΔWash-out (%)	35.19 (-91.5–66.4)	41.67 (31.8–75.0)	**0.024***

*P < 0.05, ** P < 0.01, Mann-Whitney U test. pCR, pathologic complete response; TTP, time to peak; NAC, neoadjuvant chemotherapy; MRI, magnetic resonance imaging.

Table 4. Receiver operating characteristic analysis of parameters predictive of pathological response to neoadjuvant therapy

	AUC (95% CI)	Cut-off	Sensitivity	Specificity	LR+	LR–	PPV	NPV
Baseline MTV	0.625 (0.527–0.717)	>9.92	86.49	35.21	0.75	2.61	41	83.3
Post-NAC SUV_{mean}	0.673 (0.577–0.760)	≤2.32	56.76	84.72	3.71	0.51	65.6	79.2
ΔMTV	0.645 (0.547–0.734)	>70.2	72.97	54.93	1.62	0.49	45.8	79.6
ΔSUV_{mean}	0.724 (0.630–0.805)	>30.5	81.08	56.94	1.88	0.33	49.2	85.4
ΔTLG	0.644 (0.546–0.734)	>74.6	81.08	45.07	1.48	0.42	43.5	82.1
ΔWash-out	0.635 (0.536–0.726)	>-9.52	100	38.89	1.64	0	44.3	100

< positive diagnostic test for values under the optimal cut-off > positive diagnostic test for values above the optimal cut-off, *P < 0.05. AUC, area under the curve; CI, confidence interval; LR+, positive likelihood ratio; LR–, negative likelihood ratio; PPV, positive predictive value; NPV, negative predictive value; MTV, metabolic tumor volume; TLG, total lesion glycolysis; NAC, neoadjuvant chemotherapy; SUV, standardized uptake value.

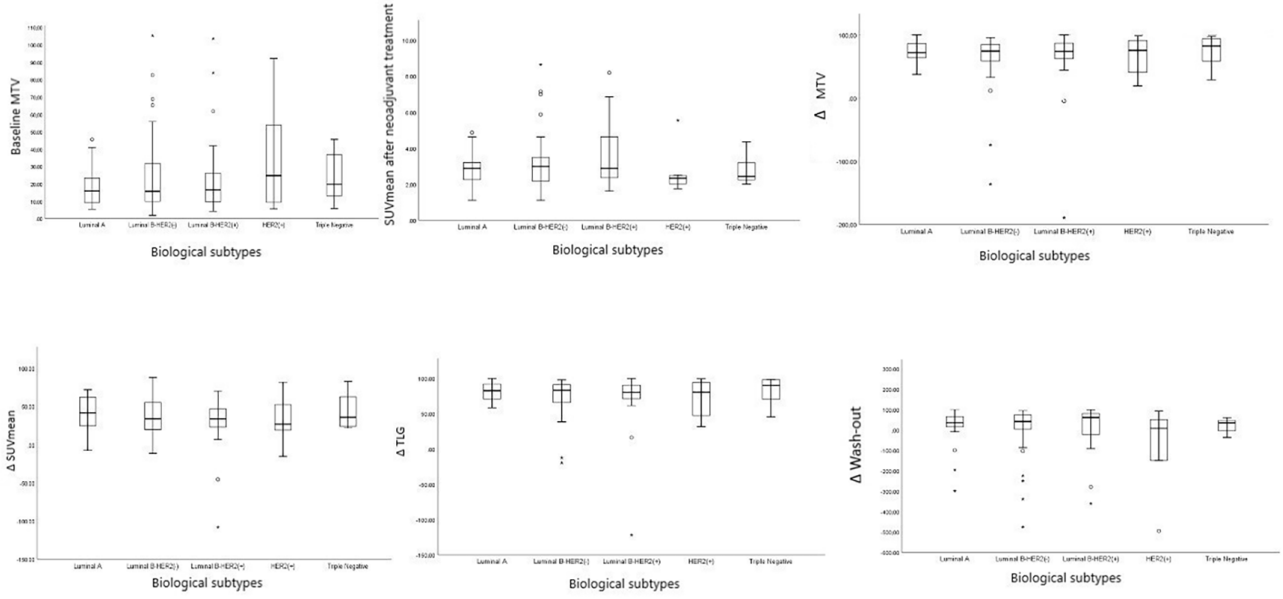

Figure 4. Baseline metabolic tumor volume, SUV_{mean} after neoadjuvant treatment, ΔMTV, ΔSUV_{mean}, ΔTLG, Δwash-out in relation to currently used biological subtypes. SUV, standardized uptake value.

NAC was not significantly associated with treatment response. In this study, the superior value of SUV_{mean} compared with MTV and TLG likely stems from its independence from tumor size, as tumor size was found to be unrelated to NAC response. The study's independent evaluation of ^{18}F-FDG PET/CT parameters and overall analysis determined ΔSUV_{mean} to be the most effective parameter for predicting NAC response.

The finding that ΔSUV_{mean} is the most significant parameter, both within the ^{18}F-FDG PET/CT parameters and overall, demonstrates that changes in tumor biology (i.e., Δ values) are the most effective predictors of response to NAC. These variations are better represented by the differences between baseline assessments and post-NAC evaluations, particularly in ΔSUV_{mean} and ΔMTV, which can predict pCR and, consequently, influence surgical procedures.

Invasive lobular carcinoma (ILC) also differs from invasive ductal carcinoma in terms of receptor expression.[29] In particular, ILC is almost always (95%) ER-positive, raising the possibility of increased utility of ER-targeting PET tracers for patients with ILC.[29] Sixteen alpha ^{18}F-fluoroestradiol is an ER-targeting PET tracer with high sensitivity and specificity for the detection of ER-positive tumors. It can be used as a predictive biomarker to demonstrate ER heterogeneity, evaluate the pharmacokinetics of ER-targeted agents, quantify residual ER during endocrine therapy, and determine the biological optimal dose of novel ER-targeted drugs.

One factor that may influence the response to systemic chemotherapy is tumor perfusion. Tumor tissue with relatively poor perfusion is believed to be less exposed to chemotherapeutic agents and therefore may not respond adequately to NAC.[29,30] This deficiency could be a factor contributing to poor responses to intravenous chemotherapy. Prior studies on large breast tumors using various techniques, including histologic analysis of vessel density, PET with ^{15}O-water, DCE-MRI, single-photon imaging with 99mTc-sestamibi, and Doppler sonography, all suggest that blood flow in LABC is highly variable.[31-33] Quantitative DCE-MRI, which assumes two chambers representing the extravascular extracellular space and blood plasma, provides absolute and thus objective measures of perfusion.[3,20,21] However, among the DCE-MRI parameters evaluated both at baseline and post-NAC in this study, only Δwash-out was able to predict the treatment response. Nevertheless, the specificity of Δwash-out was found to be significantly lower than the parameters of ^{18}F-FDG PET/CT.

Many factors may influence ^{18}F-FDG uptake into tumor cells, including the up-regulation of glucose transporters and hexokinase enzymes and neo-angiogenesis, which in turn are related to the number of viable tumor cells, their aggressiveness, and proliferative activity.[1,7,15] Angiogenesis is one of the most important of these, and one of the biggest effects of NAC drugs is that they af-

fect tumor perfusion; that is, angiogenesis. However, as shown in this study, the disruption of angiogenesis is only one of the factors affecting the tumor's pathological response. For this reason, DCE MRI parameters, whose main mechanism of action is to show tumor perfusion, show considerable variability due to the disruption of angiogenesis after neoadjuvant treatment, but do not show this pathological response. However, the main mechanism of action of PET-CT parameters is metabolic activity. Metabolic activity is higher in tumors with high perfusion/angiogenesis; however, its effect on metabolic activity, which is the main indicator of PET-CT parameters, is limited. Therefore, the rate of being affected by perfusion disorders caused by NAC drugs is limited.

Previous studies have suggested that advanced T and N stages and ER-negative status are associated with high SUV_{max} values in patients with breast cancer. Although lymph node response was not examined in this study, these parameters, which are effective in predicting the response of mass to neoadjuvant treatment, were found to be unaffected by biological subtypes.

This study had several limitations. First, the current literature describes DCE-MRI parameters using k_{trans}, v_e, and k_{ep} calculations. The authors were unable to use these parameters, since no application capable of calculating these values is available in the hospital; this can be regarded as a limitation concerning the integration of the study with existing literature. Second, FDG PET/CT was performed in the supine position, and no additional imaging was performed specifically for the position of the breasts. This may have been a misleading factor, especially in parameters such as MTV and TLG, where tumor volumes are also calculated. Some recent studies have examined the effect of breast position on PET-CT results.[34] Furthermore, the small sample size due to stringent exclusion criteria and the retrospective nature of the study were additional limitations.

In conclusion, in patients with LABC, ^{18}F-FDG PET/CT performed both at baseline and post-NAC demonstrated the metabolic changes induced by treatment. The ΔSUV_{mean} parameter is the most successful predictor of pathological response to NAC among all PET/CT parameters.

Footnotes

Conflict of interest disclosure

The authors declared no conflicts of interest.

References

1. Hyun SH, Ahn HK, Park YH, et al. Volume-based metabolic tumor response to neoadjuvant chemotherapy is associated with an increased risk of recurrence in breast cancer. *Radiology*. 2015;275(1):235-244. [Crossref]
2. Diwanji D, Onishi N, Hathi DK, et al. ^{18}F-FDG dedicated breast PET complementary to breast MRI for evaluating early response to neoadjuvant chemotherapy. *Radiol Imaging Cancer*. 2024;6(2):230082. [Crossref]
3. Akin M, Orguc S, Aras F, Kandiloglu AR. Molecular subtypes of invasive breast cancer: correlation between PET/computed tomography and MRI findings. *Nucl Med Commun*. 2020;41(8):810-816. [Crossref]
4. Waks AG, Winer EP. Breast cancer treatment: a review. *JAMA*. 2019;321(3):288-300. [Crossref]
5. Perou CM, Sørlie T, Eisen MB, et al. Molecular portraits of human breast tumours. *Nature*. 2000;406(6797):747-752. [Crossref]
6. Korde LA, Somerfield MR, Carey LA, et al. Neoadjuvant chemotherapy, endocrine therapy, and targeted therapy for breast cancer: ASCO guideline. *J Clin Oncol*. 2021;39(13):1485-1505. [Crossref]
7. Reig B, Lewin AA, Du L, et al. Breast MRI for evaluation of response to neoadjuvant therapy. *Radiographics*. 2021;41(3):665-679. [Crossref]
8. Cortazar P, Zhang L, Untch M, et al. Pathological complete response and long-term clinical benefit in breast cancer: the CTNeoBC pooled analysis. *Lancet*. 2014;384(9938):164-72. Erratum in: *Lancet*. 2019;393(10175):986. [Crossref]
9. Pace L, Nicolai E, Luongo A, et al. Comparison of whole-body PET/CT and PET/MRI in breast cancer patients: lesion detection and quantitation of ^{18}F-deoxyglucose uptake in lesions and in normal organ tissues. *Eur J Radiol*. 2014;83(2):289-296. [Crossref]
10. Pak K, Seok JW, Kim HY, et al. Prognostic value of metabolic tumor volume and total lesion glycolysis in breast cancer: a meta-analysis. *Nucl Med Commun*. 2020;41(8):824-829. [Crossref]
11. Yousefirizi F, Klyuzhin IS, O JH, et al. TMTV-Net: fully automated total metabolic tumor volume segmentation in lymphoma PET/CT images - a multi-center generalizability analysis. *Eur J Nucl Med Mol Imaging*. 2024;51(7):1937-1954. [Crossref]
12. American College of Radiology Breast Accreditation Program: Modalities. [Crossref]
13. Elston CW, Ellis IO. Pathological prognostic factors in breast cancer. I. The value of histological grade in breast cancer: experience from a large study with long-term follow-up. *Histopathology*. 1991;19:403-410. [Crossref]
14. Allred DC, Harvey JM, Berardo M, Clark GM. Prognosis and predictive factors in breast cancer by inmunohistochemical analysis. *Mod Pathol*. 1998;11:155-168. [Crossref]
15. Wang L, Luo R, Lu Q, et al. Miller-Payne grading and 70-gene signature are associated with prognosis of hormone receptor-positive, human epidermal growth factor receptor 2-negative early-stage breast cancer after neoadjuvant chemotherapy. *Front Oncol*. 2021;11:735670. [Crossref]
16. Goldhirsch A, Wood WC, Coates AS, Gelber RD, Thürlimann B, Senn HJ; Panel members. Strategies for subtypes--dealing with the diversity of breast cancer: highlights of the St. Gallen International Expert Consensus on the Primary Therapy of Early Breast Cancer 2011. *Ann Oncol*. 2011;22(8):1736-1747. [Crossref]
17. Mghanga FP, Lan X, Bakari KH, Li C, Zhang Y. Fluorine-18 fluorodeoxyglucose positron emission tomography-computed tomography in monitoring the response of breast cancer to neoadjuvant chemotherapy: a meta-analysis. *Clin Breast Cancer*. 2013;13(4):271-279. [Crossref]
18. Jiménez-Ballvé A, García García-Esquinas M, Salsidua-Arroyo O, et al. Prognostic value of metabolic tumour volume and total lesion glycolysis in ^{18}F-FDG PET/CT scans in locally advanced breast cancer staging. *Rev Esp Med Nucl Imagen Mol*. 2016;35(6):365-372. [Crossref]
19. Arici S, Karyagar SS, Karyagar S, et al. The predictive role of metabolic tumor volume on no response to neoadjuvant chemotherapy in patients with breast cancer. *J Oncol Pharm Pract*. 2020;26(6):1415-1420. [Crossref]
20. Choi EK, Yoo IR, Kim SH, Park SY, O JH, Kang BJ. The value of pre- and post-neoadjuvant chemotherapy F-18 FDG PET/CT scans in breast cancer: comparison with MRI. *Acta Radiol*. 2018;59(1):41-49. [Crossref]
21. Nguyen-Thu H, Hanaoka H, Nakajima T, et al. Early prediction of triple negative breast cancer response to cisplatin treatment using diffusion-weighted MRI and ^{18}F-FDG-PET. *Breast Cancer*. 2018;25(3):334-342. [Crossref]
22. Gerke O, Naghavi-Behzad M, Nygaard ST, et al. Diagnosing bone metastases in breast cancer: a systematic review and network meta-analysis on diagnostic test accuracy studies of 2-[^{18}F]FDG-PET/CT, ^{18}F-NaF-PET/CT, MRI, contrast-enhanced CT, and bone scintigraphy. *Semin Nucl Med*. 2025;55(1):137-151. [Crossref]
23. Kitajima K, Miyoshi Y, Yamano T, Odawara S, Higuchi T, Yamakado K. Prognostic value of FDG-PET and DWI in breast cancer. *Ann Nucl Med*. 2018;32(1):44-53. [Crossref]
24. Lee SM, Bae SK, Kim TH, et al. Value of 18F-FDG PET/CT for early prediction of pathologic response (by residual cancer burden criteria) of locally advanced breast cancer to neoadjuvant chemotherapy. *Clin Nucl Med*. 2014;39(10):882-886. [Crossref]

25. An YS, Kang DK, Jung Y, Kim TH. Volume-based metabolic parameter of breast cancer on preoperative 18F-FDG PET/CT could predict axillary lymph node metastasis. *Medicine (Baltimore)*. 2017;96(45):8557. [Crossref]

26. Capobianco N, Meignan M, Cottereau AS, et al. Deep-learning ^{18}F-FDG uptake classification enables total metabolic tumor volume estimation in diffuse large B-Cell lymphoma. *J Nucl Med*. 2021;62(1):30-36. [Crossref]

27. Wen W, Xuan D, Hu Y, Li X, Liu L, Xu D. Prognostic value of maximum standard uptake value, metabolic tumor volume, and total lesion glycolysis of positron emission tomography/computed tomography in patients with breast cancer: a systematic review and meta-analysis. *PLoS One*. 2019;14(12):0225959. [Crossref]

28. El-Galaly TC, Villa D, Cheah CY, Gormsen LC. Pre-treatment total metabolic tumour volumes in lymphoma: does quantity matter? *Br J Haematol*. 2022;197(2):139-155. [Crossref]

29. Ulaner GA, Jhaveri K, Chandarlapaty S, et al. Head-to-head evaluation of 18F-FES and 18F-FDG PET/CT in metastatic invasive lobular breast cancer. *J Nucl Med*. 2021;62(3):326-331. [Crossref]

30. Vercellino L, Cottereau AS, Casasnovas O, et al. High total metabolic tumor volume at baseline predicts survival independent of response to therapy. *Blood*. 2020;135(16):1396-1405. [Crossref]

31. Chen W, Zhu L, Yu X, Fu Q, Xu W, Wang P. Quantitative assessment of metabolic tumor burden in molecular subtypes of primary breast cancer with FDG PET/CT. *Diagn Interv Radiol*. 2018 Nov;24(6):336-341. [Crossref]

32. Im HJ, Bradshaw T, Solaiyappan M, Cho SY. Current methods to define metabolic tumor volume in positron emission tomography: which one is better? *Nucl Med Mol Imaging*. 2018;52(1):5-15. [Crossref]

33. Higuchi T, Fujimoto Y, Ozawa H, et al. Significance of metabolic tumor volume at baseline and reduction of mean standardized uptake value in ^{18}F-FDG-PET/CT imaging for predicting pathological complete response in breast cancers treated with preoperative chemotherapy. *Ann Surg Oncol*. 2019;26(7):2175-2183. [Crossref]

34. Kupik O, Tuncel M, Özgen Kıratlı P, et al. Value of dynamic 18F-FDG PET/CT in predicting the success of neoadjuvant chemotherapy in patients with locally advanced breast cancer: a prospective study. *Mol Imaging Radionucl Ther*. 2023;32(2):94-102. [Crossref]